

THE SENSITIVITY OF PRECOOLED AIR-BREATHING ENGINE PERFORMANCE TO HEAT EXCHANGER DESIGN PARAMETERS

HELEN WEBBER^{1*} ALAN BOND² AND MARK HEMPEL¹⁺

1. *Department of Aerospace Engineering, University of Bristol, Queens Building, University Walk, Bristol, BS8 1TR, UK.*

*Email: helen.webber@bristol.ac.uk

+Email: mark.hempell@bristol.ac.uk

2. *Reaction Engines Ltd, Building D5, Culham Science Center, Abingdon, Oxon, OX14 3DB, UK.*

Email: alan.bond@reactionengines.co.uk

The issues relevant to propulsion design for Single Stage To Orbit (SSTO) vehicles are considered. In particular two air-breathing engine concepts involving precooling are compared; SABRE (Synergetic Air-Breathing and Rocket Engine) as designed for the Skylon SSTO launch vehicle, and a LACE (Liquid Air Cycle Engine) considered in the 1960's by the Americans for an early generation spaceplane. It is shown that through entropy minimisation the SABRE has made substantial gains in performance over the traditional LACE precooled engine concept, and has shown itself as the basis of a viable means of realising a SSTO vehicle. Further, it is demonstrated that the precooler is a major source of thermodynamic irreversibility within the engine cycle and that further reduction in entropy can be realised by increasing the heat transfer coefficient on the air side of the precooler. If this were to be achieved, it would improve the payload mass delivered to orbit by the Skylon launch vehicle by between 5 and 10%.

Keywords: Precooled air-breathing engine, heat exchanger, LACE, SABRE, Skylon, SSTO.

1. INTRODUCTION

A reusable Single Stage to Orbit (SSTO) vehicle is essential to greatly reduce specific launch costs, and make space far more accessible. However, a pure chemical rocket reaching orbit with a practical single stage vehicle is a very marginal possibility.

In the past the likely candidate air-breathing propulsion systems considered for performance augmentation of a pure rocket system (for the purposes of SSTO) have been turbo-ramjets, scramjets and Liquid Air Cycle Engine (LACE) engines [1].

The turbojet alone employs active compression and therefore has the advantage of accelerating a vehicle from zero forward speed. The ramjet employs 'ram' compression of the intake airflow and therefore does not have this capability. The turbojet, although exhibiting a highly desirable specific impulse at low mach numbers, is limited in performance above Mach 2 as a result of high stagnation temperatures reducing the inlet mass flow and achievable pressure ratio. The turbo-ramjet combination, however, would allow further vehicle acceleration by spilling the airflow into a bypass ramjet duct at higher speeds. This system is limited up to speeds of around Mach 6, above which the net thrust falls off due to the effects of dissociation. Since the ramjet has no active compressor the intake efficiency must be very high, and an accelerating launch vehicle thus requires a variable geometry intake. This added complexity significantly increases the mass of the ramjet, and consequently the dead weight to be carried into orbit. The overall

thrust/weight (T/W) ratio of the turbo-ramjet is therefore poor due to the combined weight of the two systems and operation at low pressures.

Scramjets (supersonic combustion ramjets) avoid dissociation effects by only partially slowing the flow, limiting the static temperature rise, and combusting supersonically. This allows a much higher mach range than the ramjet. Due to its moderate combustor temperature rise and pressure ratio, however, scramjets require a large air mass flow in order to give adequate T/W ratio, and are realistically limited to well below Mach 15, the net vehicle specific impulse falling to below that of a rocket at higher Mach numbers. Apart from the problems associated with injection of hydrogen fuel at hypersonic speeds and the complex variable intake with flow stability problems, a scramjet requires an initial accelerator engine to take the vehicle up to its operational hypersonic speeds, and a rocket engine to complete the ascent into orbit. Many studies including the ESA 'Winged Launcher Configuration Study' [1] have been unable to demonstrate a positive payload for a scramjet powered SSTO vehicle.

A range of air-breathing engines and their operational envelopes are listed in Table 1. For comparison the performance characteristics of a liquid hydrogen/liquid oxygen (LH/LOX) chemical rocket is also shown.

None of the turbojet, ramjet and scramjet combinations above have a T/W ratio that is remotely able to accelerate a SSTO vehicle through its air-breathing ascent with sufficiently reduced rocket ΔV to compensate the additional weight of the air-breathing system and provide a viable payload margin. A different approach is needed.

This paper was presented at the 57th International Astronautical Congress, Valencia, Spain, October 2006. IAC-06-D2.P.2.07.

| NOTATION | | | |
|-----------------|---|----------------------|---|
| Symbols: | | | |
| A | Heat transfer surface area | m^2 | T Temperature K |
| C | Capacity rate | W/K | $\Delta \bar{T}_{ln}$ Logarithmic mean temperature difference K |
| F | Correction factor to rate of heat transfer equation | | U Overall heat transfer coefficient W/(m ² K) |
| h | Specific enthalpy | J/kg | ΔV Separation velocity m/s |
| h^* | Heat transfer coefficient | W/(m ² K) | Greek letters: |
| I_{sp} | Specific Impulse | s | γ Ratio of specific heats |
| k | Tube thermal conductance | W/mK | η_{KE} Intake kinetic energy efficiency |
| K | Capacity rate ratio | | Subscripts: |
| \dot{m} | Mass flow rate | kg/s | a Air |
| M | Mach number | | c Cycle |
| P | Pressure | N/m ² | f Final |
| \dot{Q} | Rate of heat transfer | W | h Hydrogen |
| S_{gen} | Total cycle entropy generation | J/K | he Helium |
| s | Specific entropy | J/(kgK) | i Initial |
| t | Tube thickness | m | o Total |
| | | | r Recovered |
| | | | ref Reference |

TABLE 1: Engine Performance Envelopes, Quoted I_{sp} are Fully Expanded Values. Data from [2].

| Engine | Mach range | Installed I_{sp} (s) | Installed T/W (N/kg) |
|--------------------------|------------|------------------------|----------------------|
| LH/LOX | | | |
| Rocket (vac) | 0 – 27 | 450 – 475 | 60-80 |
| Ramjet (LH) | 1 - 6 | 1500 – 3000 | 1 - 3.5 |
| Scramjet | 4 – 15 | 1000 – 3000 | 0.5- 2 |
| Turbojet | 0 - 2.5 | 2000 – 6000 | 1 – 4 |
| Precooled Engine: | | | |
| - LACE | 0 - 6 | 600 – 1000 | 6 – 14 |
| - SABRE | 0 - 5.5 | 1500 – 3200 | 6 – 14 |

The LACE engine is one variant of an overall class of air-breathing engines known as ‘precooled engines’. These are active compression engines but overcome the Mach number limitation of the turbojet by ‘precooling’ the air prior to compression. In doing so, far greater compression ratios can be achieved, enabling a vehicle to be propelled from static sea level conditions up to Mach 5 with T/W ratios 3 to 4 times that of the turbojet or ramjet. In addition, by operating at a high pressure ratio in air-breathing mode, the same rocket combustion chamber, nozzle and pumps can be used for both the air-breathing and rocket modes of operation. This minimises the mass penalty of the air-breathing turbomachinery and removes the base drag penalty of unused nozzles.

The LACE, whilst offering good T/W up to Mach 5, exhibits inadequate specific impulse due to its inherently high fuel flows. This can be avoided, however, by a redesign of the precooled engine concept using an optimised thermodynamic cycle, and is the design principle behind the Reaction Engine’s Ltd deeply precooled (non-liquefying) SABRE engine.

A twenty year study and technology development centred on the HOTOL [3] and Skylon [4] vehicles has been able to show that deeply precooled air-breathing engines combined with a rocket mode of operation for the later stages of ascent are able to offer a viable means of achieving a SSTO vehicle with adequate payload margin; the performance gained from the higher specific impulse in the air-breathing phase offsetting the impact of the increased dry mass on the rocket phase.

This paper outlines the thermodynamic design approach behind the deeply precooled engine concept and explains why this class of engine is critically dependant on the performance of the heat exchangers that cool the incoming air. Heat exchangers of the performance required for Skylon’s SABRE engine are now close to beginning trials. While these tests will demonstrate the current state of the art, further development to improve the heat transfer per kilogram is possible. A sensitivity analysis is thus provided to highlight what the potential gains in payload could be should further improvements be made in precooler performance.

2. PRECOOLED ENGINE ANALYSIS

Precooled engines, in the form of LACE, were first proposed in the 1960’s as a propulsion concept for use in the United State’s ‘Aerospaceplane’ project. Jeffs and Beeton [5] describe two such engine concepts; the straight LACE and the Oxygen Condensation system.

The straight LACE engine uses liquid hydrogen fuel to liquefy the incoming air prior to its compression and subsequent combustion in a rocket combustion chamber. The required fuel flow for this engine, however, is dictated by the precooler ‘pinch point’, whereby the hydrogen fuel must have sufficient thermal capacity to absorb the enthalpy equal to the latent heat of condensation of air at its saturated conditions.

Since the temperature rise of the hydrogen is limited to the saturated temperature of air, the mass flow of hydrogen must therefore increase to achieve the required capacity rate. Table 1 highlights that the installed specific impulse is barely double that of a LH/LOX rocket engine at its peak, and therefore unable to achieve the necessary reduction of the ΔV to be installed in rocket mode.

The Oxygen Condensation system attempts to avoid the high fuel flows of the LACE by operating a ‘turbo-ramjet’ throughout the air-breathing mode and using the cooling capacity of liquid hydrogen to liquefy only part of the airflow in a separate air-scoop system. A liquid oxygen separator would subsequently store this oxygen for later use in rocket mode. In this way high fuel flows are only required during operation of the air-scoop system and the vehicle take-off mass is reduced. However, a practical solution for achieving a viable lightweight and efficient liquid oxygen separator has yet to be found and without this the system expends a great deal of fuel in the air collection phase negating the potential advantages of the concept.

In the 1980’s the HOTOL concept transformed the design principles behind the precooled engine. This precooled engine derivative (the 1980’s RB545 [3 & 6] and the current SABRE [4] design) bypasses the need to liquefy the air and in doing so avoids the pinch point, resulting in a much reduced fuel/air ratio. Compared to the LACE this engine makes a far more efficient split between the cooling and work demands of the cycle and is a result of using entropy minimisation in the design approach for the engine cycle.

Thermodynamically, entropy is a measure of the potential of a system to convert heat energy into work and many proposed engines can be examined rigorously as to their feasibility by careful consideration of entropy changes within their cycle. A perfect engine would have no net entropy change, whilst an impossible one would have a net entropy fall.

Precooled engines for SSTO applications have to integrate with a later rocket operation phase and it is necessary to operate in airbreathing mode at high combustion pressures to achieve the high propulsive efficiency, which makes the complication worthwhile. Thus within the airbreathing engine cycle increasing the pressure of the air reduces its entropy, as does cooling it prior to compression. This decrease must be balanced by entropy increases elsewhere in the cycle since it can be regarded as an open flow isolated system. Part of the engine cycle is driven by work transfer and part by heat transfer.

Within any isolated system the entropy must increase or remain constant according to the second law of thermodynamics. An increase indicates a permanent loss of useful energy within the cycle. In the case of the LACE engine the hydrogen fuel flow is employed purely as a coolant to liquefy the incoming air, the resulting work capacity gained in heating the hydrogen stream being far greater than is needed to run the liquid air turbocompressor. Heat is thus transferred without realising the work that it is capable of and energy is therefore wasted. The liquefaction process itself represents a significant source of irreversible entropy rise, and the cycle has lost this potential also to produce work. The SABRE engine resolves this problem by cooling the air to just above its vapour boundary, reducing the required fuel flow but still providing sufficient work capacity to drive the now gaseous air turbocompressor. The SABRE thus provides similar T/W ratio to the LACE whilst maintaining high net vehicle specific impulse to over Mach 5.

The aim of the following engine cycle calculations for both the generic straight LACE (where entropy is not considered) and the deeply precooled SABRE engine (where entropy is minimised) is to illustrate the importance of considering the impact of entropy on the overall engine performance. The comparison is made for similar flight conditions and combustion chamber delivery pressure, and the resultant engine performance given in terms of equivalence ratio (where the equivalence ratio is the ratio of the actual fuel/air ratio to the stoichiometric fuel/air ratio) and net specific impulse. The SABRE engine cycle performance calculation initially considers an isentropic cycle in order to fully emphasise the potential of entropy minimisation.

Following the air-breathing phase both engines would revert to a pure rocket mode in order to complete the ascent into orbit. The rocket mode engine performance is not analysed in this paper but is assumed to be similar for both the LACE and SABRE cycle and hence does not deter from the conclusions drawn from the air-breathing engine mode comparison.

2.1 LACE Performance Calculation

Consider the flight condition of Mach 5 (since this is close to the highest achievable air-breathing Mach number for precooled engines) at 600 kts Equivalent Air Speed (EAS). We can calculate the local ambient air pressure P_a via:

$$EAS = \sqrt{\frac{\gamma_a P_a}{\rho_{sl}}} M \tag{1}$$

where ρ_{sl} is the standard sea level density of 1.225 kg/m³, and hence determine the corresponding ideal total air pressure. The ratio of recovered total pressure, P_{o_r} , in the intake, to the ideal total pressure, P_o , can be approximately represented over a wide Mach number range by the relation:

$$\frac{P_o}{P_{o_r}} = \left[1 + (1 - \eta_{KE}) \frac{(\gamma - 1)}{2} M^2 \right]^{\frac{\gamma}{\gamma - 1}} \tag{2}$$

where η_{KE} is the kinetic energy efficiency of diffusion and is typically 0.9 to 0.96 [7]. This gives a recoverable total pressure in the engine intake of just over 5 bar. The air then flows through the air liquefier where it is cooled and liquefied at a saturation temperature corresponding to the recovered intake pressure. At this temperature (97K), the corresponding latent heat of vaporization of air is approximately $\Delta h_a = 177$ kJ/kg (for notation see page 189).

Assuming the tanked hydrogen fuel is at 20 K and 1 bar, subsequent compression to 200 bar at 80% isentropic efficiency would give a delivery temperature of approximately 33.7 K. The enthalpy change of hydrogen from delivery conditions to 97 K is thus $\Delta h_h = 887$ kJ/kg.

The ratio of the latent heat of air at its saturated conditions to that of the available enthalpy of hydrogen (determined by its delivery conditions and the air saturated temperature) defines the ‘pinch point’ and hence the corresponding minimum fuel/air ratio,

$$f/a,$$

required:

$$\frac{f}{a} = \frac{\Delta h_a}{\Delta h_h} \quad (3)$$

This gives a pinch point fuel/air ratio of 0.205 or an equivalence ratio of approximately 7.

Unlike energy, entropy is not conserved and throughout the above heat transfer process some 7000 Js/(kgK) of entropy rise occurs (see Equation 5). The liquid may now be pumped to 200 bar using a conventional cycle for combustion at 150 bar. The work required to compress the liquid air is assumed negligible.

At lower Mach numbers the intake recovery pressure is reduced and consequently the saturation temperature of air is reduced causing its latent heat of condensation to increase as well as limiting the specific enthalpy rise of the hydrogen. As a result, at lower stagnation pressures the fuel/air ratio for the LACE engine is increased substantially, highlighting the necessity for LACE engines to have highly efficient intakes. At higher Mach numbers metal temperature limitations on the air liquefier set the minimum required fuel/air ratio. However, for the LACE operating up to Mach 5 the controlling performance factor is the intake recovery pressure.

2.2 SABRE (Isentropic) Performance Calculation

By considering the thermodynamics of an engine cycle, for the same flight conditions and combustion chamber delivery pressure the SABRE precooled engine can achieve a far lower fuel/air ratio. In this cycle the air remains gaseous and the hydrogen is used as a heat sink for the heat engine rather than purely as a coolant. In doing this, sufficient work can be produced to compress the air stream whilst minimising the required fuel flow, and is a direct result of minimising the entropy generation within the cycle.

To illustrate the SABRE concept, consider a ‘black-box’ precooled engine cycle as an open isolated system as shown in Fig. 1. The entropy change within the isolated system equals the sum of the entropy changes as a result of all the irreversibilities of the system components [8]. These irreversibilities are due to friction and heat transfer across finite temperature differences within the cycle.

Irreversibilities within the cycle will thus include; machine inefficiencies, pressure losses in pipes due to skin friction, turbulence within the compressors and turbines, heat exchanger temperature differences, temperature limitations, and those due to real fluid properties. The efficiency and ultimate feasibility of the precooled engine concept thus relies heavily on the ability to reduce the total entropy generation of the system.

The respective enthalpy and entropy balances between the air and hydrogen streams for the open isolated system shown in Fig. 1 are:

$$h_{a_f} - h_{a_i} = \frac{\dot{m}_h}{\dot{m}_a} (h_{h_f} - h_{h_i}) \quad (4)$$

and,

$$\frac{\dot{S}_{gen}}{\dot{m}_a} = s_{a_f} - s_{a_i} + \frac{\dot{m}_h}{\dot{m}_a} (s_{h_f} - s_{h_i}) \quad (5)$$

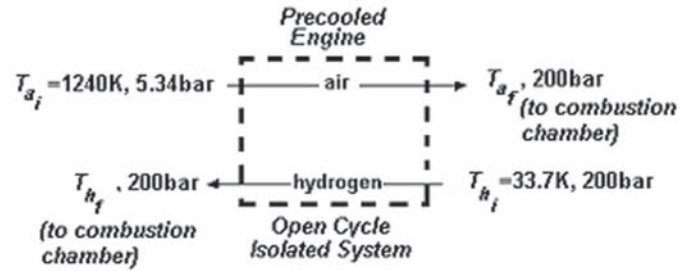


Fig. 1 Black box precooled engine cycle diagram.

where, S_{gen} , is the entropy increase of the isolated system due to irreversibilities. In order to gain maximum work from the cycle the outlet temperatures for the air and hydrogen must be equal, otherwise a further heat engine could be added across the outlets. The overall entropy generated must be positive or equal to zero for the engine cycle to obey the laws of thermodynamics, and the minimum fuel/air ratio is thus achieved when the entropy increase is zero.

Using Equations (4) and (5), and referring to the hydrogen and air inlet conditions, as defined in Fig. 1 and in the LACE performance calculation, we can determine the fuel/air ratio for a given value of cycle entropy generation. For an isentropic cycle $S_{gen} = 0$, and assuming the air must be compressed to 200 bar for combustion at 150 bar, this corresponds to outlet temperatures of 896 K and a fuel/air ratio of 0.0293. This is approximately an equivalence ratio of 1. Thus by using the heat available to drive the cycle and balancing the entropy fall of the air with the entropy rise of the hydrogen stream we can obtain a very high performance engine cycle.

2.3 Performance Comparison

Table 2 gives a comparison of the analysed LACE and SABRE performance characteristics. A real SABRE engine will of course be non-isentropic and entropy will increase as a result of irreversibilities in the cycle, corresponding to an increase in the required fuel flow or reduction in achievable pressure ratio. Hence a comparison is also made with a real SABRE cycle model where the turbomachinery, combustor, heat exchangers and air inlet performance are analysed using Reaction Engine’s software. For the combustion performance a NASA code for equilibrium combustion by McBride, Reno and Gordon [9] is used. It should be noted that for the LACE engine the hydrogen exiting the air liquefier is cool enough (approx. 480 K) to be used for combustion chamber and jacket cooling, and this will slightly reduce the fuel/air ratio quoted in Table 2. In the real (non-isentropic) SABRE engine the compressed air outlet temperature must be limited to 700 K and the hydrogen to 876 K so that the respective nozzle jacket cooling and film cooling of the combustion chamber can be implemented in air-breathing mode. This factor is included in the quoted performance for the real SABRE cycle. For each case the intake momentum drag is evaluated in order to provide the net specific impulse.

As shown in Table 2, even the quoted non-isentropic SABRE cycle performance in air-breathing mode is a substantial improvement over the LACE engine cycle. The difference between the current SABRE performance status and the isentropic case illustrates the scope in further improving the engine performance by reducing the irreversibilities of the engine cycle.

TABLE 2: Precooled Air-Breathing Engine Performance Characteristics for Flight Condition Mach = 5, EAS = 600 kts and a Pressure Recovery Factor of 0.3.

| | LACE | SABRE (Isentropic) | SABRE: (non-isentropic) |
|-----------------------------------|-------|-----------------------|----------------------------|
| Hydrogen/Air Equivalence Ratio | 0.205 | 0.0293 | 0.0818 |
| Chamber Pressure, bar | 7 | 1 | 2.8 |
| Net I _{sp} (s) | 150 | 150 | 103 |
| | 990 | 5145 | 1838 |

3. THE SABRE CYCLE

Figure 2 shows a simplified SABRE cycle. In air-breathing mode the SABRE engine operates similarly to a Brayton cycle whereby heat is extracted from the inlet air flow via a precooler, producing work to drive the compressor and rejecting heat to the hydrogen stream. A closed helium power loop is interposed between the hot air-stream and cold hydrogen stream such that better thermal capacity matching is achieved in the heat exchangers. This also avoids hydrogen embrittlement in the precooler tubes and provides a barrier between the hydrogen and air, amongst other factors.

In the air-breathing mode air is cooled to a temperature above its vapour boundary (140 K), prior to compression up to 145 bar, 700 K. The hot air then divides and flows to the main combustion chamber and the fuel rich preburner. The hot exhaust from the preburner passes through HX3 and raises the helium temperature from the precooler to a constant value of 1180 K to provide the turbine with constant operating conditions. In this way the turbomachinery operates at virtually constant flow conditions. The hydrogen fuel delivered by the hydrogen pump is initially used to cool and recompress the helium before passing to the preburner. In transition to rocket mode the air intake closes, the compressor is run down and the preburner combustion temperature is reduced since only the work to drive the turbopumps and helium circulator is now required.

During operation in air-breathing mode, the largest source of irreversibility within the SABRE cycle (upstream of the combustion chamber) is that due to the heat transfer through the precooler. The following analysis outlines how an improvement in the heat transfer coefficient of the precooler could reduce the entropy generation and thus greatly improve upon the performance of the current SABRE engine quoted above.

4. PRECOOLER PERFORMANCE

Irreversibilities within a heat exchanger are caused by entropy rise due to heat transfer over a finite temperature difference and also that due to the pressure loss through the system. These must be minimised whilst achieving the required heat transfer rate using as small a heat transfer area as possible.

The rate of heat transfer, \dot{Q} , per unit heat transfer area, A , between two fluids separated by a solid boundary can be expressed as:

$$\frac{\dot{Q}}{A} = U \Delta T \tag{6}$$

where ΔT is some mean temperature difference between two

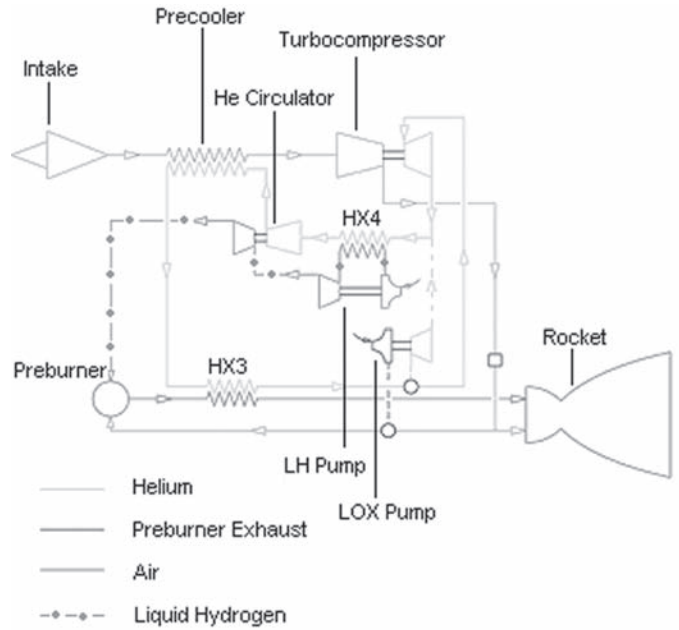


Fig. 2 Simplified SABRE cycle, HX = heat exchanger.

fluids exchanging heat, and U is overall heat transfer coefficient. The reciprocal of U is the overall thermal resistance of the heat exchanger and is expressed by:

$$\frac{1}{U} = \frac{1}{h_a^*} + \frac{t}{k} + \frac{1}{h_{he}^*} \tag{7}$$

here

$$\frac{1}{h_a^*}$$

is the air flow thermal resistance,

$$\frac{1}{h_{he}^*}$$

is the helium flow thermal resistance, and

$$\frac{t}{k}$$

is the resistance of the separating solid surface where t is the material thickness and k the material conductance. Since the conductance of the solid boundary is generally far greater than either of the fluid heat transfer coefficients, the overall heat transfer coefficient is controlled by the most thermally resistive fluid layer – the air in this case.

In order to maximise

$$\frac{\dot{Q}}{A}$$

we can enhance the heat transfer coefficient of the fluid layers by, for example, increasing the fluid flow velocity. For low density gaseous flow heat exchangers, however, an increase in flow velocity can have an overall negative effect on performance due to the much greater increase in frictional power loss [10].

These factors begin to indicate the necessary design parameters for the SABRE precooler. The requirement for low mass flux necessitates a large number of flow channels, manifesting itself in a large frontal area heat exchanger. Given the relatively low achievable heat transfer coefficients of the gaseous precooler, a very large heat transfer area is necessary in order to achieve the 400 MW power requirement at the Mach 5 design condition. This ultimately leads to a ‘compact heat exchanger’ design such that the heat exchanger volume does not become excessive, and where the ‘compactness’ or ‘high surface area density’ is achieved by reducing the diameter of the flow passages. It can be shown that extended heat transfer surfaces, i.e. in the form of fins on each of the flow channels, which do not help to contain the pressure differential, are not mass effective. Given the high internal pressure of the helium coolant, the flow channels must be of tubular form in order to minimise weight. The precooler configuration therefore consists of a compact array of small diameter circular tubes.

Compactness in itself gives rise to improved heat transfer per unit area since the fluid heat transfer coefficient is inversely proportional to the tube diameter [10]. Fluid flow heat transfer coefficients can also be increased by interrupting the surface boundary layers to prevent their growth in thickness. A cross flow arrangement of the precooler tubes therefore automatically forces new boundary layers to grow on each tube.

As previously outlined, large irreversibilities also manifest themselves in the finite temperature potential that drives the heat transfer between the hot air stream and helium coolant stream. ΔT can be minimised firstly by introducing a counterflow design into the heat exchanger. Figure 3 illustrates the geometry of the cross-counterflow arrangement used on the SABRE precooler.

The section of precooler illustrated in Fig. 3 is made up of a series of modules such as the prototype shown in Fig. 4. These are set at shallow sweep angles to the external air flow such that the cross flow element is preserved.

Figure 5 shows the 0.9 mm circular tubes brazed into the headers that form the inlet and outlet of each module. Helium coolant within the tubes of each module follows a spiral path from inlet to outlet such that a counterflow arrangement is also achieved. The precooler is made up of several of these large diameter compact annular cross-counterflow matrices such that a large frontal area is seen by the air and the low mass flux is achieved.

There are two regions within the SABRE precooler, however, where the remaining finite temperature difference between the hot airstream and the helium coolant causes a very large irreversibility. These exist at both the hot end of the precooler where a large temperature difference is caused by

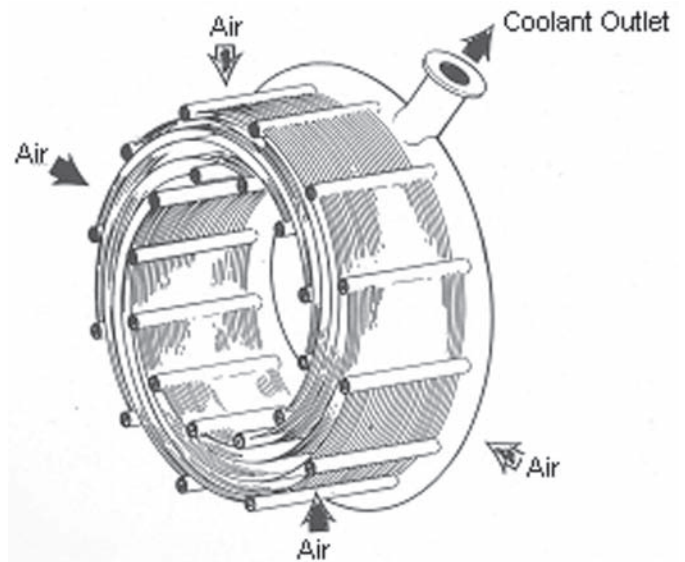


Fig. 3 Section of SABRE cross-counterflow precooler.

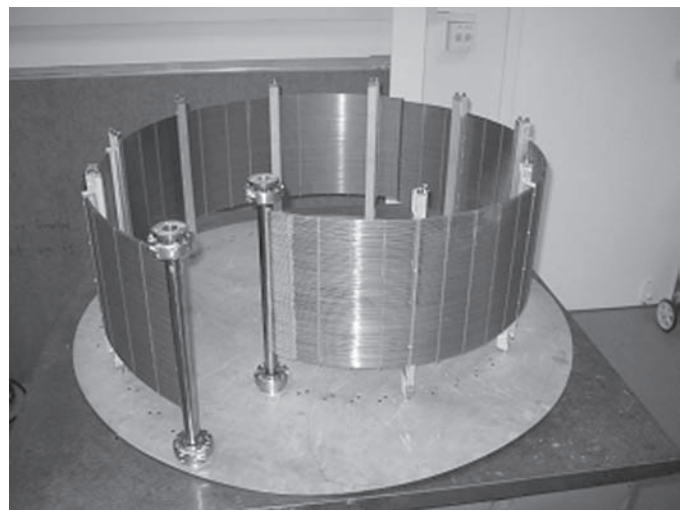


Fig. 4 First prototype precooler module.

precooler material temperature limitations and also at the cold end of the heat exchanger where the finite temperature difference is larger relative the lower average temperature at the cold end.

4.1 ΔT Due to Material Temperature Limitations

At the Mach 5 design condition air enters the engine at 1240 K (real gas properties). Due to precooler material constraints, however, the helium coolant is limited to 950 K and the potential entropy generation as a result of this large temperature difference must be controlled by increasing the capacity rate of the coolant flow.

When considering a counterflow heat exchanger with no imposed temperature limitations the entropy generation can be minimised by matching the capacity rates of both streams. Given the above temperature limitations at entry to the precooler, the entropy generation can be reduced by increasing the helium coolant capacity rate; the higher coolant mass flow allows the heat to be transferred at a higher average temperature.

Figure 6 illustrates that a capacity ratio (helium/air) of 3

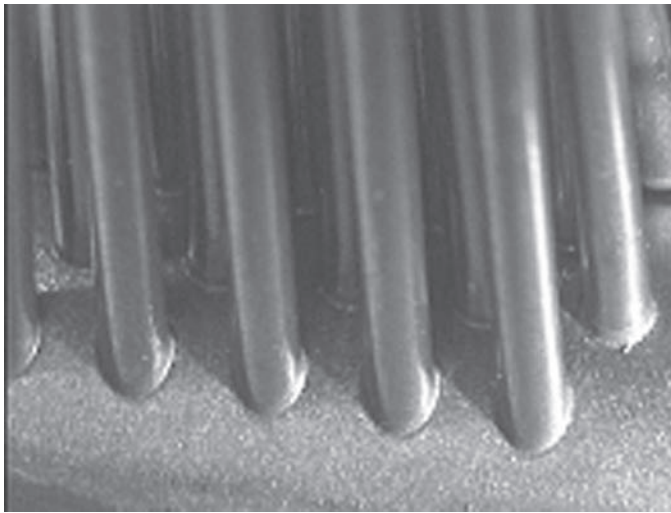


Fig. 5 Pre-cooler tubes brazed into module headers.

must be employed such that the entropy increase in the hot end of the heat exchanger is considerably reduced.

The pre-cooler is thus split into two parts. At the hot end a non-isentropic counterflow heat exchanger with a capacity ratio of 3 is used in order to counteract the entropy rise due to the hot end temperature limitation of the pre-cooler.

T_2 , as indicated in Fig. 6 and Fig. 7, is the resulting cold end temperature of the non-isentropic counterflow heat exchanger. The remaining heat in the external air flow can then be removed using a low temperature heat exchanger that is not constrained by material temperature limitations and can therefore operate closer to isentropic conditions. Figure 7 illustrates the initial counterflow heat exchanger using an increased capacity rate ratio (K_1) followed by a capacity matched counterflow heat exchanger (K_2).

The very nature of low temperature heat transfer, however, constitutes a major source of entropy generation even at the lower ΔT 's achieved using a capacity matched counterflow arrangement. Since the low temperature heat exchanger must still remove almost 60% of the heat from the intake air flow, the performance of this heat exchanger, in terms of the ability to reduce ΔT , is critical to the performance gain of the whole engine cycle.

4.2 ΔT Due to Low Temperature Heat Exchange

For the pre-cooler capacity matched counterflow heat exchanger (see Fig. 8) where C is the capacity rate

$$\dot{m}c_p$$

of either the air or helium stream, the entropy rise per unit capacity rate,

$$\frac{\Delta S}{C},$$

assuming no pressure loss is given by:

$$\frac{\Delta S}{C} = \ln\left(\frac{T_3}{T_2}\right) + \ln\left(\frac{T_2 - \Delta T}{T_3 - \Delta T}\right) \quad (8)$$

Assuming a $\Delta T \ll T_2, T_3$, Equation (8) can be reduced to:

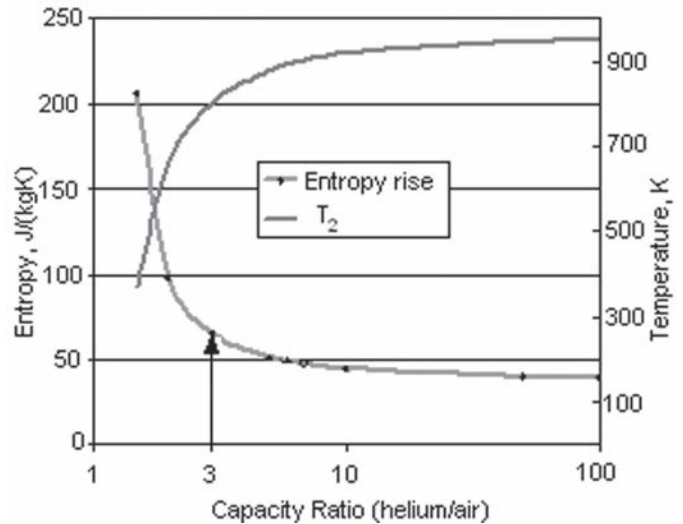


Fig. 6 The Effect of helium to air capacity ratio on entropy generation in a counterflow heat exchanger with air inlet temperature of 1240 K and helium exit temperature of 950 K, and where T_2 is the cold end temperature of both streams assuming no ΔT .

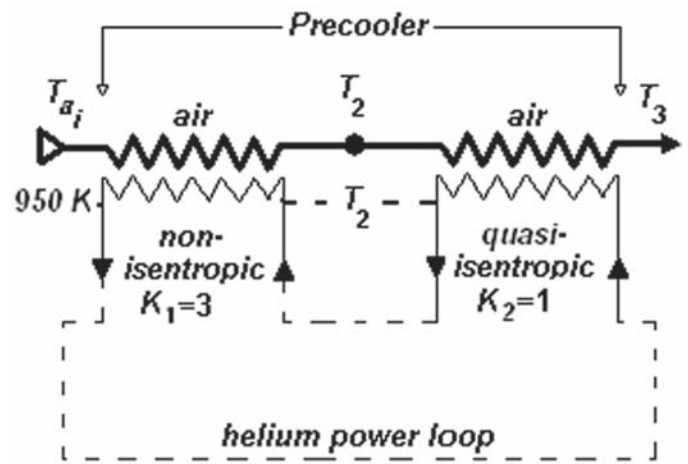


Fig. 7 Pre-cooler thermodynamics; K in this case is the helium to air capacity ratio.

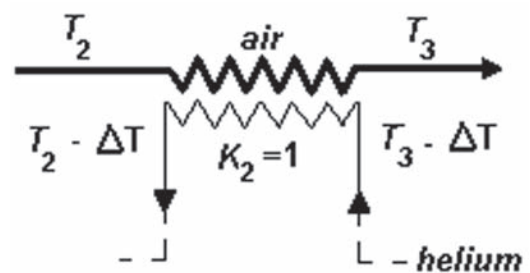


Fig. 8 Pre-cooler low temperature, capacity matched heat exchanger.

$$\frac{\Delta S}{C} \approx \frac{(T_2 - T_3)}{T_2 T_3} \Delta T \quad (9)$$

The entropy increase of the pre-cooler low temperature heat exchanger is therefore proportional to the finite temperature difference, ΔT , between the hot air stream and helium coolant stream.

4.2.1 ΔT Sensitivity Analysis

Considering again the enthalpy and entropy balance of the air and hydrogen streams as outlined in Fig. 1, and assuming no pressure loss within the hydrogen stream, the maximum achievable air pressure ratio,

$$\frac{P_{a_f}}{P_{a_i}}$$

is defined by:

$$\frac{P_{a_f}}{P_{a_i}} = \left[\frac{\left(\frac{T_{a_i} + K_c T_{h_i}}{1 + K_c} \right)^{(1+K_c)}}{T_{a_i} T_{h_i}^{K_c}} \right]^{\frac{\gamma_a}{\gamma_a - 1}} \exp \left(- \frac{\gamma_a}{\gamma_a - 1} \frac{S_{gen}}{m_a c_{p_a}} \right) \quad (10)$$

Since

$$S_{gen} = \sum_{n=i}^{n=1} \Delta S_i$$

where ΔS_i is the entropy increase of a single component in the engine cycle, we can assess the sensitivity of each individual component's performance on overall cycle performance.

Substituting Equation (9) into Equation (10) gives the engine cycle fuel/air capacity ratio, K_c , as a function of the low temperature heat exchanger ΔT for a given air compression ratio. This is referenced to the ΔS performance of the low temperature heat exchanger and the current fuel/air capacity ratio of 1.2 of SABRE.

We can thus determine the mass of fuel saved in air-breathing mode as a result of a reduced ΔT across the precooler low temperature heat exchanger; the reduced ΔT reducing the entropy rise and allowing the same amount of compression work to be done for a smaller fuel flow. Ultimately, for every tonne of fuel saved in air-breathing mode this corresponds to almost a quarter tonne of payload gain into orbit.

Figure 9 illustrates the percentage payload gain into orbit as a result of the saving in fuel flow in air-breathing mode due to the reduced ΔT in the low temperature heat exchanger. Since a heat exchanger's heat transfer rate is proportional to U , A and ΔT (see Equation (6)), a reduction in ΔT is achieved by a direct increase in heat exchanger surface area, or an equivalent increase in the heat exchanger heat transfer coefficient, for the same rate of heat transfer. Hence the payload gain into orbit, as shown in Fig. 9, is given as a function of increased precooler surface area or, correspondingly, an increase in precooler heat transfer coefficient. The increase in precooler area and precooler heat transfer coefficient is referenced respectively to the current SABRE precooler area A_{ref} and heat transfer coefficient U_{ref} .

The limit of achievable payload gain is where the heat exchanger ΔT tends to zero and the performance approaches isentropic conditions. This is seen approaching 13% on Fig. 9.

It can be seen that doubling the heat transfer area or heat transfer coefficient of the low temperature precooler results in a

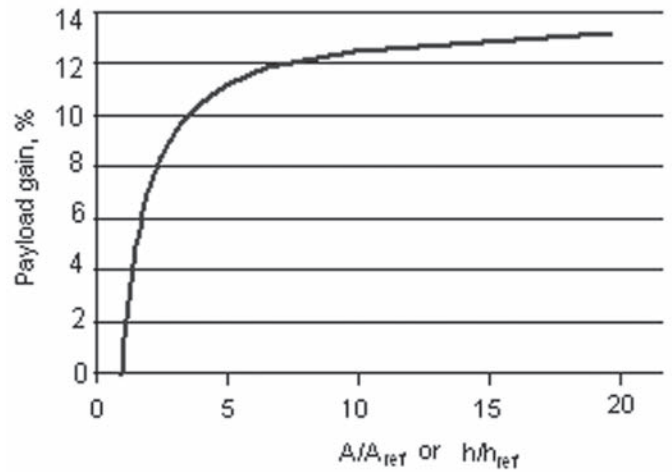


Fig. 9 A maximum possible payload gain of 13% is theoretically achieved as the performance of the precooler low temperature heat exchanger approaches that of an isentropic heat exchanger.

significant gain in payload. Increasing either A or U by a factor of 2.5 shows an additional 1 tonne in payload on top of the current Skylon SSTO 12 tonne payload capability to Low Earth Orbit.

However, the precooler matrix mass is currently approximately 1 tonne, and increasing the heat exchanger surface area will increase the precooler mass also by roughly 1 tonne, adding no overall net gain to the vehicle performance. Increasing the area is therefore clearly not a way forward.

The key to substantially furthering the gain in payload is to improve the overall heat exchanger heat transfer coefficient, U , without significantly impacting on the irreversibility due to pressure loss, or the mass due to added features.

The conductance of the matrix tube wall is far greater than the convective conductance of the hot air stream and helium coolant stream, and has negligible effect on the overall heat transfer coefficient. The thermal capacity of helium is also much greater than that of air and the overall increase in heat transfer coefficient is therefore governed by that achievable of the air side heat transfer coefficient. This can in principle be achieved by modification of the flow regime around the precooler tubes, enhancing the heat transfer to the surface without detrimental increases to pressure loss.

5. CONCLUSIONS

This paper has demonstrated that the SABRE precooled engine has made substantial gains in performance over the traditional LACE precooled engine concept and has explained the reasons for believing that the SABRE engine will make a SSTO vehicle viable.

By designing the engine from a thermodynamic point of view, and minimising the entropy generation within the cycle, the SABRE has been able to make a far more efficient split between the cooling and work demands on the engine cycle. In terms of performance this has achieved almost double the net specific impulse of the LACE. Further advances in performance are possible if the entropy generation within the current SABRE cycle can be further reduced.

The largest source of irreversibility within the SABRE cycle (upstream of the combustion chamber) is that due to heat transfer through the precooler. Analysis has shown that these irreversibilities can be reduced if means can be found to moderately increase the heat transfer coefficient on the air side of the precooler. This has the potential to increase the

payload capability of the Skylon SSTO reusable launch vehicle by a further tonne. This attractive prospect has inspired a research programme that is focused on enhancing the air side heat transfer of the SABRE precooler by several possible means. This programme will be the subject of future publications.

REFERENCES

1. "Winged Launcher Configuration Study", ESA Contract No. 7379/87/NL/FG, 1993.
2. R. Varvill and A. Bond, "A Comparison of Propulsion Concepts for SSTO Reusable Launchers", *JBIS*, **56**, pp.108-117, 2003.
3. B.R.A. Burns, "HOTOL space transport for the twenty first century", Proceedings of the Institute of Mechanical Engineers, *Part G – Journal of Aerospace Engineering*, **204**, pp.101-110, 1990.
4. R. Varvill and A. Bond, "The Skylon Spaceplane", *JBIS*, **57**, pp.22-32, 2004.
5. R.A. Jeffs and A.B.P. Beeton, "Liquid Air Cycle Engines for High-speed Aircraft", *JBIS*, **19**, pp.484-490, 1964.
6. M. Hempzell, "HOTOL's Secret Engines Revealed", *Spaceflight*, **35**, pp.168-172, 1993.
7. G.L. Dugger in W.H.T. Loh (Ed) "*Jet, Rocket, Nuclear, Ion and Electric Propulsion: Theory and Design*", Springer-Verlag, New York; 1968.
8. G. Rogers and Y. Mayhew, "Engineering Thermodynamics: Work and Heat Transfer", Prentice Hall, Fourth Edition 1992.
9. J.B. McBride, M.A. Reno and S. Gordon, "CET93/PC: Chemical Equilibrium with Transport Properties", COSMIC PROGRAM # LEW-16017, 1993.
10. W.M. Kays and A.L. London, "Compact Heat Exchangers", Krieger Publishing Company, Florida, Reprint Edition with corrections, 1998.

(Received 6 March 2007; 29 March 2007)

* * *